RSC Advances

PAPER

View Article Online
View Journal | View Issue

Cite this: *RSC Adv.*, 2016, **6**, 4634

Performance enhancement in ZnO nanowire based double Schottky-barrier photodetector by applying optimized Ag nanoparticles†

Xin Zhao,[ab] Fei Wang,*[a] Linlin Shi,[ab] Yunpeng Wang,[a] Haifeng Zhao[a] and Dongxu Zhao*[a]

Received 29th September 2015
Accepted 22nd December 2015

DOI: 10.1039/c5ra20161f

www.rsc.org/advances

In this work, a UV photodetector made of a ZnO nanowire with double Schottky Barrier (SB) contacts was fabricated by an electric field guided assembly process. Then the Ag-nanowire composite in the device was achieved through an RF metal sputtering method. Under 5 V bias, the values of responsivity and photoconduction gain of the final device could reach up to 4.91×10^6 A W^{-1} and 1.67×10^7, respectively. Surprisingly, the device covered with optimized Ag nanoparticles still presented its spectrum selectivity in the visible-blind band. The nonlinear behavior at small bias was governed by the reversely biased SB contacts. After introducing Ag nanoparticles, the localized surface plasmon resonance (LSPR) induced absorption could account for the enhanced performance. In addition, the increased dark current was attributed to the involuntary introduction of localized gating effect near the contacts.

Introduction

Nowadays, ultraviolet (UV) photodetectors of different materials and mechanisms are widely used in various applications such as flame detection, environmental monitoring, chemical sensing, optical communication and so on.[1] In order to improve both the sensitivity and integration level, nanoscale semiconductors were later synthesized and used to fabricate UV photodetectors.[2,3] ZnO nanostructures, which have attracted much attention due to their excellent properties such as large bandgap energy of 3.37 eV and exciton binding energy of 60 meV at room temperature,[4] are the ideal materials in constructing light-emitting diodes, optically pumped lasers and light radiation sensors in the UV band.[5] Since the first report of a ZnO nanowire based optical switch was presented by Kind *et al.*,[6] a large number of works had been reported for improving both the sensitivity and reset time. For example, Zhou *et al.* reported that the UV sensitivity of nanosensor was improved by four orders of magnitude and the reset time was reduced from several hundreds of seconds to about 0.8 s by utilizing Schottky contact.[7] Meanwhile, it had emerged out that nano-photodetectors combined with metal particles could induce plasmonics enhancement in the device. From the report by Muhlschlegel *et al.* in 2005, a nanometer-scale gold dipole antenna was fabricated to resonate at optical frequencies.[8] It opened up the era of linking propagating radiation and enhanced optical fields together, which meant metallic nanoparticles could be settled as sub-wavelength antennas to couple more light radiation into semiconductors through plasmonic near-field mode.[9] Gogurla *et al.* had proved that the photoresponse of Au–ZnO nanocomposites can be effectively enhanced by 80 times, and the sensing response of Au–ZnO nanocomposites were enhanced both in UV and visible region.[10] However, the observed sensitivity was higher in the visible band because of the localized surface plasmon resonance (LSPR) effect of Au NPs, which resulted in a poor spectrum selection for the UV photodetector. A similar report of carbon nanotube (CNT) photodetectors enhancement was reported by Zhou *et al.* that the photocurrent enhancement of more than 3 times was achieved by the strong local plasmonic resonance of Au nanoparticles with a peak around 631 nm.[11] So the UV photodetector with higher performance and spectrum selectivity is needed to be investigated further.

In this work, Ag nanoparticles covered ZnO nanowire photodetectors with double SB contacts were fabricated by electric field guided assembly and simple metal sputtering methods to avoid the disadvantages mentioned above. Based on previous report by Jiang *et al.*, there are two resonances peaks at around 350 and 500 nm for Ag nanoparticles, which are the quadrupole and dipole modes, respectively.[12] Therefore, we chose Ag nanoparticles as the nanoantennas working in local electric field coupling mode rather than scattering and waveguide manner. The device assembled by the decorated nanowire

[a]*State Key Laboratory of Luminescence and Applications, Changchun Institute of Optics, Fine Mechanics and Physics, Chinese Academy of Sciences, 3888 Dongnanhu Road, Changchun 130021, People's Republic of China. E-mail: wangf@ciomp.ac.cn; zhaodx@ciomp.ac.cn*

[b]*University of the Chinese Academy of Sciences, Beijing 100049, People's Republic of China*

† Electronic supplementary information (ESI) available. See DOI: 10.1039/c5ra20161f

exhibits improved photocurrent of 178.15 μA under relatively weak UV illumination of 1.67 mW cm^{-2} at 365 nm. That means the responsivity and photoconduction gain could reach the values of 4.91×10^6 A W^{-1} and 1.67×10^7, respectively.

Experiment

In our ZnO nanowire synthesis process, the growth mechanism was governed by the VLS–VS hybrid growth mode.[13–15] This process of synthesizing ZnO nanowires took place in the horizontal CVD furnace tube. Briefly, the alumina boat that contained the mixture of ZnO and graphite powder, together with the substrate, were transferred into the heating zone. The Ar gas flow was maintained at 200 sccm for about 10 min, then turned to 100 sccm. At this point, the temperature was raised to 925 °C at a rate of 50 °C min^{-1}. After about 40 min of reaction, the furnace was cooled to room temperature. The dark gray or white product could be observed on the substrate.

Electric field guided assembly of ZnO nanowire is the most feasible and lowcost way to accomplish the device containing only one or a few nanowires compared to other assembly methods in sub-micro scale.[16–19] Fig. 1 shows the schematic illustration of electric field assisted assembly facility. Several counter electrode patterns on glass with 5 μm gaps and 10 μm widths were made by conventional lithography technique. The assembled device is presented in the inset image of Fig. 1. Different sized Ag nanoparticles attached to the surface of the conducting channel mentioned in this paper were deposited by plasma sputtering coating machine, and each type of the Ag nanoparticles was synthetically regulated by the particular sputtering time. The detailed synthesis and construction steps along with the extra experiments to check the structure quality and chemical composition of the synthesized ZnO nanowire and ZnO–Ag heterostructure were presented in the ESI† part.

After growth, the synthesized ZnO nanowires were examined for its morphology and growth quality *via* scanning electron microscopy (SEM) HITACHI-S4800. Photoluminescence (PL) character of the nanowire was also investigated by using a 325 nm He–Cd laser illumination system of JY-630 micro-Raman spectrometer. A 365 nm GaN LED combined with DC voltage supplier and an adjustable holder were served as UV lighting source, and its light density could be easily controlled through applying proper voltages. The electrical properties including current–voltage (*I*–*V*) characteristics and time dependent photocurrent were measured by using the HP1500A Semiconductor Device Analyzer at room temperature. The spectral responsivity was obtained by a home-built phase-lock amplifier based measurement system with a 150 W xenon arc lamp light source.

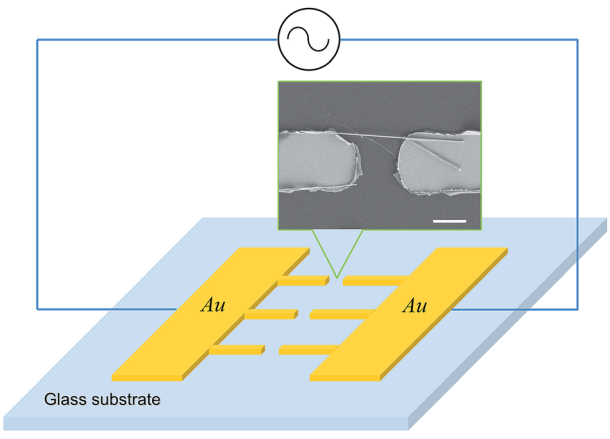

Fig. 1 Schematic view of electric field assisted assembly for ZnO nanowire photodetector. The inset shows the SEM image of the fabricated device.

Results and discussion

The SEM images of ZnO nanowires synthesized on the Si substrate are shown in Fig. 2. Fig. 2a shows the synthesized nanowire array, and it is clear that the nanowires possess sharp edges and uniform morphology. These well aligned nanowires grow along the [0001] direction, which reveals that the *c*-axis is the preferred growth direction for a ZnO nanowire.[20–22] Fig. 2b is the enlarged picture of a single nanowire. The length of the product is in the scale of several tens of micrometers with

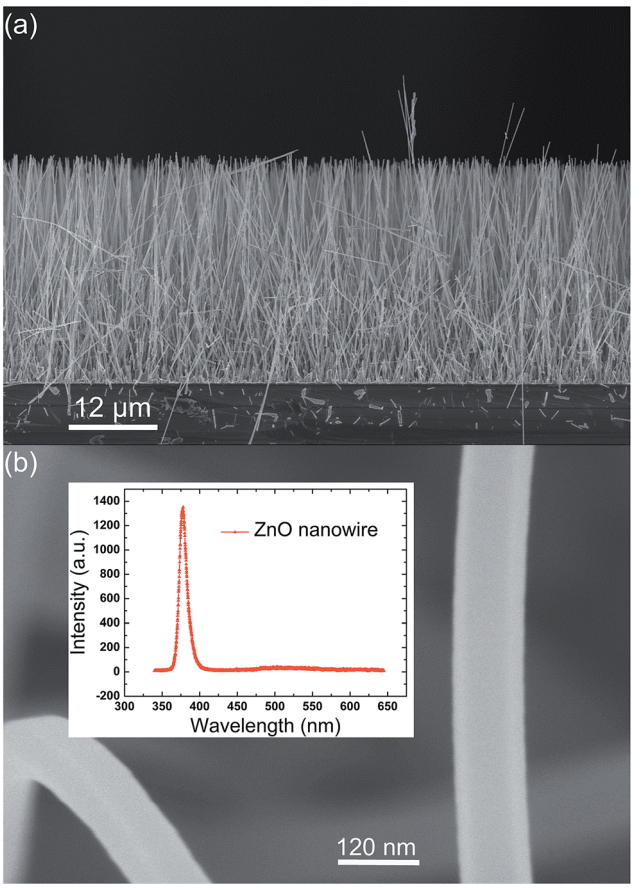

Fig. 2 SEM images of the synthesized ZnO nanowires. (a) Cross-sectional SEM image of the nanowires, (b) close view of the nanowire. The inset of (b) shows the PL spectra of the ZnO nanowire array at room temperature.

relatively uniform diameter at about 70 nm. For a further examination to the quality of the ZnO nanowire, room-temperature PL spectrum measurement was taken under a 325 nm He–Cd laser illuminating system. The inset in Fig. 2b is the PL spectra obtained from the synthesized nanowire. Under the exciting of the incident photons, strong near band-edge UV emission with peak position at 378 nm is observed and little deep-level emission appears. The UV emission peak has a full width at half-maximum (FWHM) of 10.8 nm. At low excitation power, this narrow FWHM value and low ratio between UV and visible light intensity in the PL spectrum are the indexes of high quality ZnO nanowires.

Ag nanoparticles with average diameter of 10 nm were uniformly dispersed on a ZnO nanowire surface, as shown in Fig. 3a. Each island like Ag nanoparticle has outstanding hemisphere profile, which is separated by about 10 nm gap. In the scattering experiment, it is apparent that the scattering efficiency for the island like nanoparticles increases while the particle size extending to the range of about 150 nm.[23,24] But the short coming is obvious that the over broaden absorption spectrum located in the longer wavelength band and the red shift of plasmonic resonance peaks would both appear as the particle size growing, which is not welcome in the UV spectrum photodetector design.[25] Also, over extended Ag nanoparticles could lead to a larger dark current in our device structure. So it is possible to utilize the smaller ones to construct the UV sensor to couple most of the total light into the semiconductor because of the enhanced local surface plasmonic electromagnetic field.[26] Fig. 3b shows the optical absorption spectra of Ag nanoparticles in three sizes (10 nm, 20 nm and 30 nm), which presents a red shift in the plasmonic resonance band when increasing the particle size. There are two absorption peaks through the UV-vis band, one in UV band and the other in visible band. The peaks at 356 nm and 427 nm on the absorption curve of the smallest one are associated with the quadrupole and dipole plasmonic resonance band of Ag nanoparticles in atmosphere environment.[26,27] Generally, the particles here work like little antennas to receive the incident light power and couple the energy of local plasma resonance field into the semiconductor *via* near-field plasmonic wave, especially when the wavelength of the incident light locates nearby the peak position of the plasmonic resonance spectrum of Ag nanoparticles.

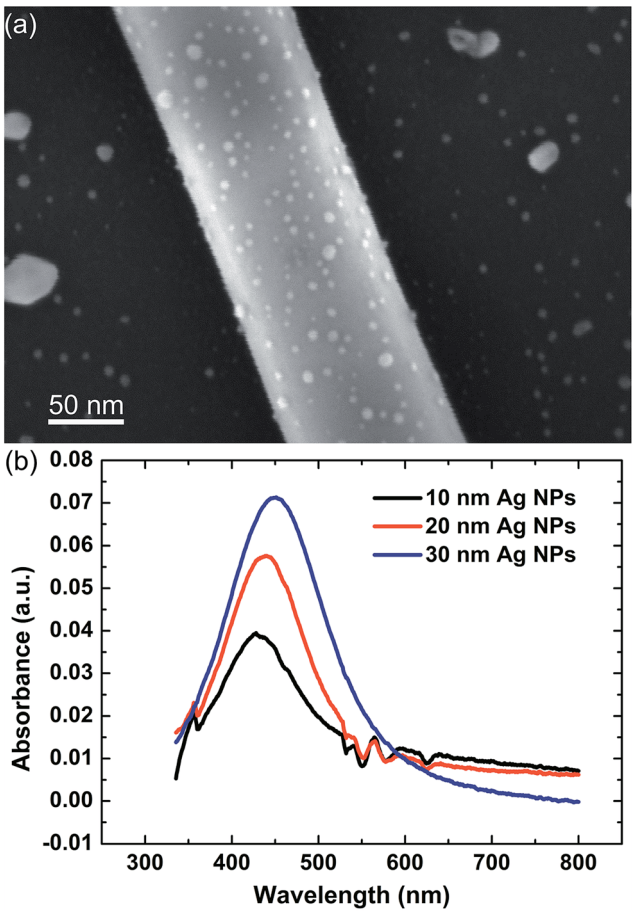

Fig. 3 Ag nanoparticles on the surface of a ZnO nanowire. (a) Close view of the Ag nanoparticles with 10 nm diameter on the nanowire surface. (b) UV-vis absorption spectra of Ag nanoparticles with three typical sizes.

The schematic image of the device is shown in Fig. 4a. The M–S–M photodetector with serial connected two back-to-back Schottky barriers (SB) in both contact areas has formed in the structure. All the experiments were carried out in air atmosphere at room temperature under the UV LED illumination system with fixed power density ($\lambda = 365$ nm, power density = 1.67 mW cm^{-2}). The *I–V* characteristics of the devices with and without Ag nanoparticles are presented in Fig. 4b. At 5 V bias condition, the photocurrent I_{ph} of the decorated device is up to 178.15 μA. The enlarged *I–V* curves for the two types of devices in the dark are presented in Fig. 4c and d. The nonlinear behavior of the device measured in the dark indicates that the SBs with different SB heights exist in the contact regions of both sides. Our device is more likely two Schottky diodes connected back to back in serial manner instead of forming a single one.[22] When the device was exposed to the UV source at power density of 1.67 mW cm^{-2}, the photocurrent I_{ph} dramatically increases from 2.92 nA to about 130 μA. The ratio of photocurrent to dark current for untreated ZnO nanowire is about 4.45×10^4. The responsivity R of a photodetector is defined as the photocurrent value I_{ph} that generated by per unit incident optical power, which is in expression of $R = I_{ph}/P_{opt}$, where $I = I_{light} - I_{dark}$, P_{opt} is the incident light power covering the nanowire surface. Furthermore, photoconduction current gain G can be expressed as the ratio of the number of collected electrons to the number of absorbed photons in unit time,[28] which is defined as

$$G = \frac{I_{ph}/q}{P_{opt}/h\nu} = \frac{R}{q/h\nu} \quad (1)$$

where q is the elementary charge, ν is the frequency of the incident photon and R is the responsivity. For the untreated nanowire device, R and G are estimated to be 3.717×10^6 A W^{-1} and 1.263×10^7, respectively. As for the detector with Ag nanoparticles, its dark current and photoresponse behaviors under UV illumination are quite different from previous reports.[29,30] The dark current at 5 V bias voltage is enlarged to

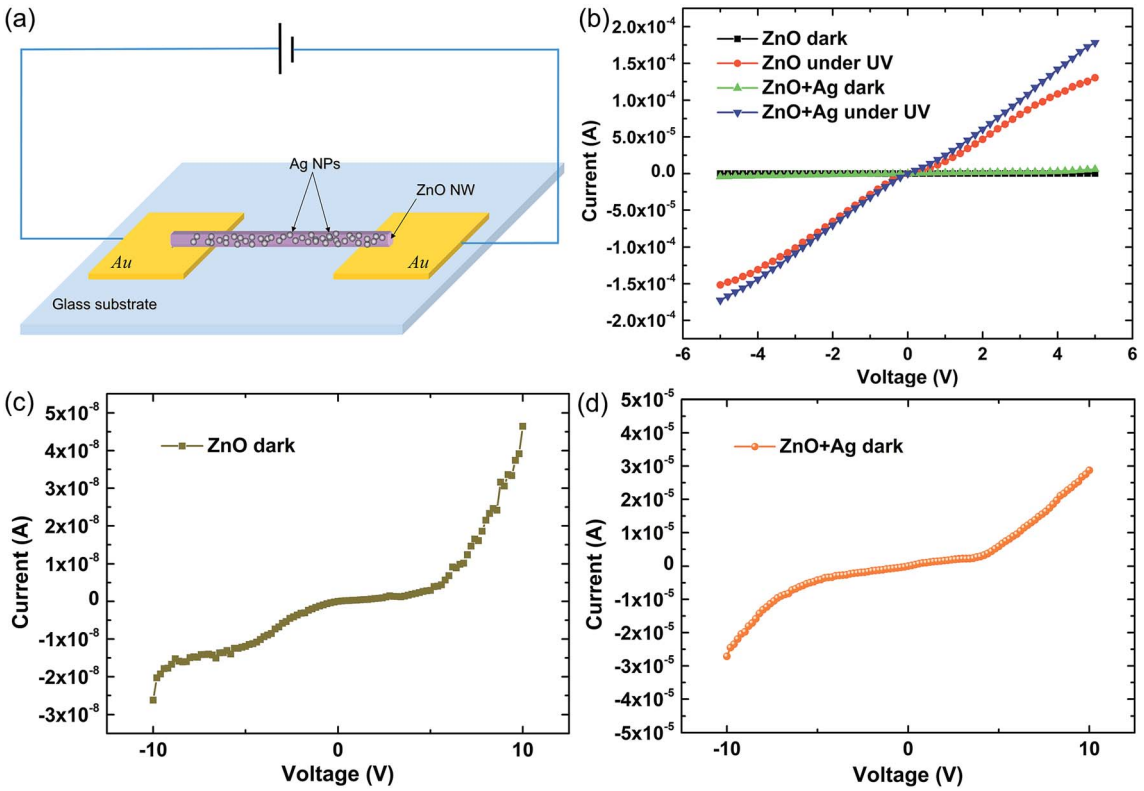

Fig. 4 (a) Schematic image of the complete device with double SB contacts. (b) *I*–*V* curves of the devices made of bare and decorated nanowires both in dark and under 365 nm UV illumination. (c) and (d) Enlarged images from (b) show the nonlinear behaviors of the devices with bare and decorated nanowires in the dark.

about 5.83 μA. Meanwhile, the photocurrent has increased to 178.15 μA as well. The values of R and G here are about 4.91×10^6 A W^{-1} and 1.67×10^7. The improvement of R and G by 32% over the untreated nanowire photodetector has been achieved. It is clear that the interaction between ZnO material and incident light was enhanced in the manner of applying Ag nanoparticles as the light harvesting antennas.

Fig. 5a shows the response behaviors of the devices with and without the Ag nanoparticles at bias of 5 V. The time-resolved photocurrents contain three UV on/off cycles, in which the turn-on time and turn-off time are 30 s and 180 s each. The rising time of the current is defined as the time spending in reaching 90% of the peak value from 10% of it, while the decay time is *vice versa*. With our carefully examination, the rising time and decay time of the device without Ag nanoparticles are 11.7 s and 28 s, respectively. When referring to the device with Ag nanoparticles, the on/off cycles possess the raising time of 6.3 s and decay time of 26.3 s. The existence of Ag nanoparticles on the surface of ZnO nanowire may contribute to the shorter photoresponse time. It seems that the built-in electric-field along the radial direction in the device with Ag nanoparticles could sufficiently suppress the recombination of photo-generated electron–hole pairs under UV light and then the saturated current could be reached in a shorter time.[31] Once the UV was turned off, the photocurrent decay was governed by the SB altering mechanism that the current recovered to the minimum once the O_2 molecules had absorbed near the contact region.[6,35] The spectral responsivity of the two types is presented in Fig. 5b. When the incident light has the energy higher than the band gap of ZnO nanowire, which is about 3.37 eV (368 nm), both detectors show a broad spectral response in visible-blind band and their cut-off edges are located at 380 nm. The identical response behavior of the both types prove that the adherent Ag nanoparticles haven't changed the intrinsically visible-blind property of the photodetector.

For the device composited of Au electrodes and ZnO nanowire, it is expected that Schottky barriers could form at the contact regions because of their work functions at 5.3 eV and 4.1 eV each. The height of the SB (ϕ_{SB}) at the interface is largely determined by the work function difference between metal and ZnO nanowire surface states induced by chemical absorption of O_2.[28,32] We choose thermionic emission diffusion theory to depict the current passing through the barrier at reverse bias when the reverse current isn't negligible in nanoscale device as follows:[27]

$$J_{TED} = A^{**}T^2 \exp\left(-\frac{q\phi_{SB}}{kT}\right)\left[\exp\left(\frac{qV}{kT}\right) - 1\right] \quad (2)$$

where A^{**} is the effective Richardson constant, k is Boltzmann constant, T is the environmental temperature, q is the elemental charge and V is the applied bias voltage. The width of the depletion layer (W_D) between the two materials is:

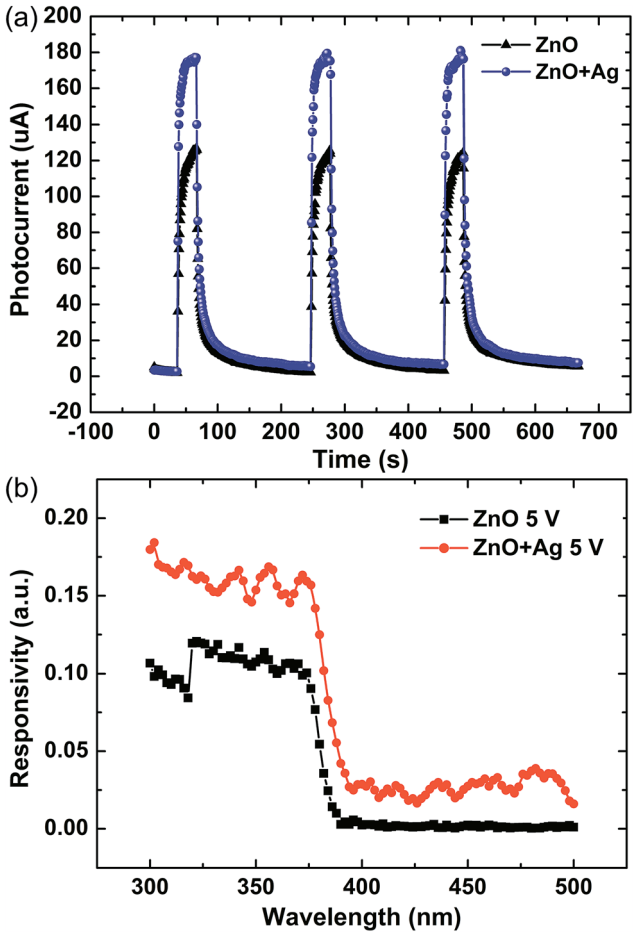

Fig. 5 (a) Time dependence of the photocurrent under multiple on/off cycles. (b) Spectral responsivity of the devices with two types of conducting channels at 5 V bias.

$$W_D = \sqrt{\frac{2\varepsilon_S}{qN_D}\left(\phi_{bi} - V - \frac{kT}{q}\right)} \quad (3)$$

where

$$\phi_{bi} = \phi_{SB} - (E_c - E_f) \quad (4)$$

ε_S is the dielectric constant, N_D is the donor concentration near the depletion layer and ϕ_{bi} is the built-in potential for metal–semiconductor interface. Deduced from the above equations, the reverse current at certain voltage is sensitive to the SB height and the relative depletion layer width. From previous reports, the local gate near the higher barrier contact have stronger influence on the current transport.[33,34] It means that the light induced electron–hole pairs, adsorbed molecules and applied electrical field at the SB contact area can enormously generate a detectable current change separately. The device working in this dominant manner is called the Schottky-gated nanosensor, as introduced before.[32]

In the dark, oxygen molecules are chemically absorbed on the ZnO nanowire surface by capturing the free electrons in the n-type semiconductor nanowire [O_2 (g) + e^- → O_2^- (ad)]. As a result, a high resistive depletion layer is formed on and beneath the surface of nanowire in several tens of nanometers scale.[35] As shown in Fig. 6a, the area of relative high concentration of positive ions presented by the dashed blue line is the depletion layer of the untreated device in dark. Under UV illumination, electron–hole pairs are generated in the body of nanowire [$h\nu$ → e^- + h^+]. Holes generated in the surface depletion layer near SB zone would probably be attracted by the O_2^- to migrate to the low electronic potential region along the built-in electric field and discharge the negative charges [h^+ + O_2^- → O_2 (g)]. The desorption of O_2 and some holes at the interface under dynamic equilibrium lower the height of SB according to the eqn (3). The thinner depletion layer is shown in the red solid line area.

When referring to the nanowire photodetector with Ag nanoparticles, the depletion layer under the nanowire surface has an asymmetry distribution in the radial direction. The phenomenon is shown in Fig. 6b. In the dark, the built-in SB between Au electrode and ZnO nanowire is formed as soon as the device was fabricated. Once Ag nanoparticles were deposited on the ZnO nanowire, the electric field strength and associated ions distribution would be rearranged because of the differences in electronegativity of the two metal materials. Free electrons of Ag nanoparticles were transported into the depletion layer, which could account for the decrease of positive ionic

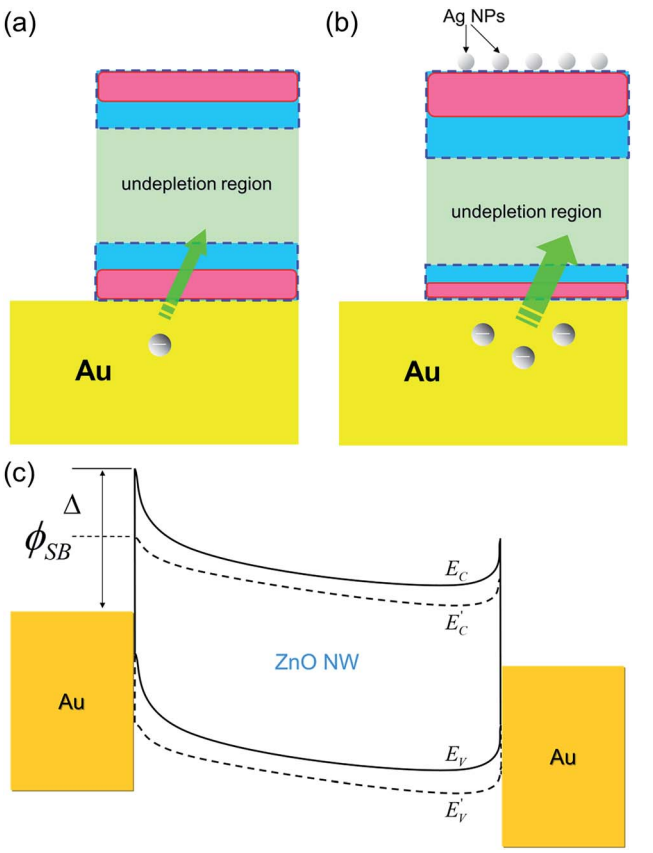

Fig. 6 (a) Bare ZnO nanowire as the conducting channel, few electrons could tunnel through the SB area. (b) Nanowire decorated with Ag nanoparticles leads to an enhanced tunneling current. (c) Schematic energy band model of the devices account for the enhanced current both in dark and under UV source.

site. Also, some of them could possibly tunnel into the Au electrode as thermion to lower the SB height. The SB region, as a result, would shrink to a thin layer. The formed thin depletion layer with asymmetric distribution is presented in the dashed blue line area. The red line area corresponds to the depletion layer when exposed to the incident UV light. So the enhanced dark current and photocurrent would tunnel through the SB region. Fig. 6c illustrates the energy band structure model of the ZnO nanowire based device which is modulated by the localized gating effect. The solid and dash lines indicate the band structures before and after the Ag deposition. A decreased SB height of Δ is introduced in after the deposition of Ag nanoparticles.

Conclusions

In summary, we have fabricated a ZnO nanowire based UV photodetector with double SB contacts using electric field guided assembly technology. Reasonable improvement could be achieved through applying uniform sized Ag nanoparticles on the ZnO nanowire surface. Under fairly low UV illumination (365 nm) density at 1.67 mW cm^{-2}, the responsivity and photoconduction gain of the decorated device could reach up to 4.91×10^6 A W^{-1} and 1.67×10^7, respectively. The enhanced performance combined with the high spectrum selectivity are believed to be associated with the enhanced surface trap states and LSPR effects from the uniform Ag nanoparticles, and the nanoparticles here play an important role in the localized gating effect induced dark current change in the nanoscale conductive channel. It is revealed that fabricating the ZnO nanosensor by electric-field assembly and Ag sputtering is a lowcost and convenience way to realize a high performance UV photodetector.

Acknowledgements

This work was supported by the National Basic Research Program of China (973 Program) under Grant No. 2011CB302004, the National Natural Science Foundation of China under Grant No. 11504367.

Notes and references

1 E. Monroy, F. Omnes and F. Calle, *Semicond. Sci. Technol.*, 2003, **18**, R33–R51.
2 Z. L. Wang, *J. Phys.: Condens. Matter*, 2004, **16**, R829–R858.
3 T. Y. Zhai, X. S. Fang, M. Y. Liao, X. J. Xu, H. B. Zeng, B. Yoshio and D. Golberg, *Sensors*, 2009, **9**, 6504–6529.
4 P. D. Yang, H. Q. Yan, S. Mao, R. Russo, J. Johnson, R. Saykally, N. Morris, J. Pham, R. G. He and H. J. Choi, *Adv. Funct. Mater.*, 2002, **12**, 323–331.
5 C. Jagadish and S. J. Pearton, *Zinc Oxide Bulk, Thin Films and Nanostructures*, Elsevier, New York, 1st edn, 2006.
6 H. Kind, H. Q. Yan, B. Messer, M. Law and P. D. Yang, *Adv. Mater.*, 2002, **14**, 158–160.
7 J. Zhou, Y. D. Gu, Y. F. Hu, W. J. Mai, P. H. Yeh, G. Bao, A. K. Sood, D. L. Polla and Z. L. Wang, *Appl. Phys. Lett.*, 2009, **94**, 191103.
8 P. Muhlschlegel, H. J. Eisler, O. J. F. Martin, B. Hecht and D. W. Pohl, *Science*, 2005, **308**, 1607.
9 H. A. Atwater and A. Polman, *Nat. Mater.*, 2010, **9**, 205–213.
10 N. Gogurla, A. K. Sinha, S. Santra, S. Manna and S. K. Ray, *Sci. Rep.*, 2014, **4**, 6483.
11 C. J. Zhou, S. Wang, J. L. Sun, N. Wei, L. J. Yang, Z. Y. Zhang, J. H. Liao and L. M. Peng, *Appl. Phys. Lett.*, 2013, **102**, 103102.
12 M. M. Jiang, H. Y. Chen, B. H. Li, K. W. Liu, C. X. Shan and D. Z. Shen, *J. Mater. Chem. C*, 2014, **2**, 56–63.
13 T. J. Kuo, C. N. Lin, C. L. Kuo and M. H. Huang, *Chem. Mater.*, 2007, **19**, 5143–5147.
14 X. F. Duan and C. M. Lieber, *Adv. Mater.*, 2000, **12**, 298–302.
15 J. Z. Zhang, *J. Phys. Chem. Lett.*, 2012, **3**, 2920–2921.
16 G. H. Yu and C. M. Lieber, *Pure Appl. Chem.*, 2010, **82**, 2295–2314.
17 A. W. Maijenburg, M. G. Maas, E. J. B. Rodijk, W. Ahmed, E. S. Kooij, E. T. Carlen, D. H. A. Blank and J. E. Elshof, *J. Colloid Interface Sci.*, 2011, **355**, 486–493.
18 B. R. Burg, *Langmuir*, 2009, **25**, 7778–7782.
19 C. S. Lao, J. Liu, P. X. Gao, L. Y. Zhang, D. Davidovic, R. Tummala and Z. L. Wang, *Nano Lett.*, 2006, **6**, 263–266.
20 Z. L. Wang, *Mater. Today*, 2004, **7**, 26–33.
21 S. Barth, F. H. Ramirez, J. D. Holmes and A. R. Rodriguez, *Prog. Mater. Sci.*, 2010, **55**, 563–627.
22 X. D. Wang, C. J. Summers and Z. L. Wang, *Nano Lett.*, 2004, **4**, 423–426.
23 S. A. MAIER, *Plasmonics: fundamentals and applications*, Springer, US, 1st edn, 2007.
24 H. R. Stuart and D. G. Hall, *Appl. Phys. Lett.*, 1998, **73**, 3815–3817.
25 S. Pillai, K. R. Catchpole, T. Trupke and M. A. Green, *J. Appl. Phys.*, 2007, **101**, 093105.
26 K. R. Catchpolea and A. Polman, *Appl. Phys. Lett.*, 2008, **93**, 191113.
27 D. W. Pohl, *Near-Field Optics and Surface Plasmon Polaritons*, Springer, Heidelberg, 2001.
28 S. M. Sze and K. N. Kwok, *Physics of Semiconductor Devices*, Wiley Interscience, 3rd edn, 2006.
29 K. W. Liu, M. Sakurai, M. Y. Liao and M. Aono, *J. Phys. Chem. C*, 2010, **114**, 19835–19839.
30 S. K. Tzeng, M. H. Hon and I. C. Leu, *J. Electrochem. Soc.*, 2012, **159**, H440–H443.
31 D. D. Lin, H. Wu, W. Zhang, H. P. Li and W. Pan, *Appl. Phys. Lett.*, 2009, **94**, 172103.
32 Y. F. Hu, J. Zhou, P.-H. Yeh, Z. Li, T.-Y. Wei and Z. L. Wang, *Adv. Mater.*, 2010, **22**, 3327–3332.
33 Z. Y. Zhang, C. H. Jin, X. L. Liang, Q. Chen and L. M. Peng, *Appl. Phys. Lett.*, 2006, **88**, 073102.
34 Z. Y. Fan and J. G. Lu, *Appl. Phys. Lett.*, 2005, **86**, 032111.
35 C. Soci, A. Zhang, B. Xiang, S. A. Dayeh, D. P. R. Aplin, J. Park, X. Y. Bao, Y. H. Lo and D. Wang, *Nano Lett.*, 2007, **7**, 1003–1009.